ACS chemical biology

Articles

pubs.acs.org/acschemicalbiology

Fluorescence Lifetime of Fluorescent Proteins as an Intracellular Environment Probe Sensing the Cell Cycle Progression

Artem Pliss,[†] Lingling Zhao,[†] Tymish Y. Ohulchanskyy,[†] Junle Qu,*[,‡] and Paras N. Prasad*[,†]

[†]Institute for Lasers, Photonics and Biophotonics, University at Buffalo, State University of New York, Buffalo, New York 14260-3000, United States

[‡]Key Laboratory of Optoelectronic Devices and Systems of Ministry of Education and Guangdong Province, Institute of Optoelectronics, Shenzhen University, 3688 Nanhai Road, Shenzhen, Guangdong Province 518060, PR China

Supporting Information

ABSTRACT: The fluorescence lifetime of fluorescent proteins is affected by the concentration of solutes in a medium, in inverse correlation with local refractive index. In this paper, we introduce the concept of using this dependence to probe cellular molecular environment and its transformation during cellular processes. We employ the fluorescence lifetime of Green Fluorescent Protein and tdTomato Fluorescent Protein expressed in cultured cells and probe the changes in the local molecular environment during the cell cycle progression. We report that the longest fluorescence lifetimes occurred during mitosis. Following the cell division, the fluorescence lifetimes of these proteins were rapidly shortened. Furthermore the fluorescence lifetime of tdTomato in the nucleoplasm gradually increased throughout the span of S-phase and remained constantly long until the end of interphase. We interpret the observed fluorescence lifetime changes to be derived from changes in concentration of macromolecular solutes in the cell interior throughout cell cycle progression.

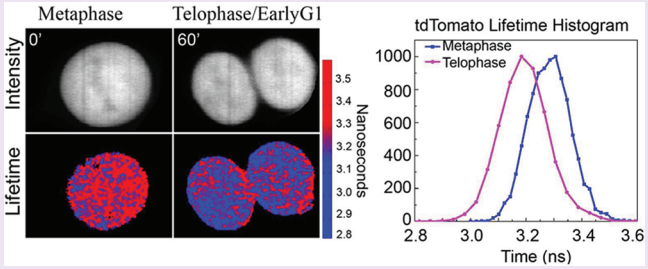

Probing of local molecular environment in cells is of significant value in creating a fundamental understanding of cellular processes and molecular profiles of diseases, as well as studying drug cell interactions. A number of spectroscopic and time-sequenced imaging approaches have been utilized for this purpose.[1] Recently we showed the utility of an integrated biophotonic imaging coupled with Raman spectroscopy to study the molecular environment and its transformations during cellular processes.[2,3] In this report we demonstrate that fluorescence lifetime of intracellular fluorescent proteins can be used as a valuable probe for monitoring of the cell-cycle-dependent changes in the cellular molecular environment.

In recent years a growing number of studies have been dedicated to characterization of biomolecular properties of nucleoplasm, the liquid content of the cell nucleus. The nucleoplasm represents a viscous medium abundant in organic and inorganic solutes, which diffuse and freely interact, participating in regulation of cellular functions.[4−6] The molecular content of nucleoplasm is continuously balanced by a complex interplay of timely coordinated synthesis and degradation of macromolecules as well as by a gradual decrease in their concentration, caused by growth of the nuclear volume throughout the interphase of the cell cycle.[6−11] The biomolecular properties of the cell nuclear interior have been investigated by a number of techniques such as motion tracking of nanoparticles or small fluorescent molecules,[12−14] interferometry,[15] and probing of mechanical deformations of the cell nucleus.[16] An interesting approach was taken by Choi *et al.*, who developed a high resolution tomographic phase microscopy for mapping of refractive index in live cells and tissues.[17] These methods, however, are not fully adequate for studies of the nucleoplasm, due to inability to analyze it separately from the nuclear structure−function compartments and chromatin domains, which are immersed in the nucleoplasm but have a different molecular composition.[2,15,18−20]

Here we illustrate the use of the fluorescence lifetime of fluorescent proteins (FPs) as a probe for monitoring of nucleoplasm saturation with macromolecular solutes. FPs are unique naturally fluorescent macromolecules, cloned from several marine organisms. Despite differences in their origin, the basic structure of various FPs is nearly identical, featuring a fluorophore embedded inside a rigid, barrel-shaped domain.[21,22] Biomedical applications of FPs include probing of molecular interactions *via* fluorescence lifetime imaging (FLIM).[1,23−28] In this technique the fluorescence lifetime (τ) in every pixel of the acquired image is determined as a function of radiative and nonradiative pathways of fluorophore transition from excited to the ground level, as described by the equation $1/\tau = k_r + k_{nr}$, where k_r and k_{nr} are the radiative and nonradiative decay rates, respectively; k_r is known to be a function of the local refractive index.[29] The relation between fluorescence lifetime, τ, and the refractive index in the

Received: February 13, 2012
Accepted: May 17, 2012
Published: May 17, 2012

fluorophore's vicinity, n, is described by the Strickler–Berg equation:[30]

$$1/\tau = 2.880 \times 10^{-9} n^2 \frac{\int I(\tilde{\nu})\, d\tilde{\nu}}{\int I(\tilde{\nu})\tilde{\nu}^{-3}\, d\tilde{\nu}} \int \frac{\varepsilon(\tilde{\nu})}{\tilde{\nu}}\, d\tilde{\nu}$$

where I is the fluorescence emission intensity, ε is the extinction coefficient, and $\tilde{\nu}$ is the wavenumber. The fluorescence lifetime of FPs in solution was experimentally shown to be modulated by change of the concentration of solutes in the fluorophore medium, in accordance with an inverse dependence of τ on the square of refractive index of the medium, in agreement with the Strickler–Berg formula.[24,31,32] This dependence was later used to probe a complex intracellular environment in both fixed and live cells.[33,34] Furthermore, little has been reported on the sensitivity of the lifetimes of FPs to other than refractive index factors in the cellular environment, in the absence of fluorescence quenchers.[32] It should be discussed. however, that FPs' spectral characteristics are known to depend on pH.[35−37] This dependence is based on difference in absorption and fluorescence of the anionic and neutral forms of the FP chromophores. Equilibrium between these forms is changed together with pH, resulting in corresponding changes in absorption and fluorescence.[35] For GFP, the neutral form of the fluorophore (absorption/emission at ∼400/470 nm, correspondingly) is progressively converted to the anionic form (absorption maximum at ∼490 nm) as the pH increases. This causes an increase in the intensity of fluorescence from the anionic form peaked at ∼510 nm. The reported pH indicators (ratiometric and nonratiometric) based on different FPs mutants undergo similar conversion from weaker fluorescent neutral form absorbing at shorter wavelengths and to an anionic form absorbing at longer wavelength and producing more intense fluorescence.[35,38] At the same time, in contrast to the fluorescence intensity, which was unambiguously determined by the amount of the anionic GFP fluorophore, the lifetime of GFP fluorescence was shown to not be sensitive to the change in pH.[36]

Interestingly enough, in another study[39] an application of FLIM of enhanced GFP to intracellular pH measurement has been developed. Utilizing the difference in excitation/emission spectra of neutral and anionic forms of the GFP fluorophore, Nakabayashi and coauthors used an excitation at 405 nm and monitored emission at 510−515 nm to measure the fluorescence lifetime response to changing pH. As a result, they determined a pH dependence of the average lifetime, defining it from a mixture of decays of neutral and anionic fluorophores. However, if the excitation is in the range where only an anionic fluorophore absorbs (*e.g.*, 470−480 nm), the pH dependence is not measurable.[36] Furthermore, the lifetime changes in the interval of the physiologic intranuclear pH (7−7.5) were shown to be insignificant even with 405 nm excitation.[39] We thus agree with a concept that the fluorescent lifetime of intracellular FPs can be used as a probe of local refractive index in the cell interior,[33,34] as a significant input of other factors in the measured value of τ is not expected.

In diverse biological applications the link existing between the refractive index and fluorescence lifetime opens the way for sensitive probing of concentration of macromolecular solutes (*e.g.*, proteins), whose contribution to overall refractive index of the cell nucleus is much higher than that of small organic and inorganic molecules and ions in the cell interior. In this context, FPs are optimal nucleoplasmic probes, as in mammalian cells they are not participating in specific molecular interactions and also not recruited to the nuclear structure−function compartments, and thus the changes in FPs fluorescence lifetime would specifically reflect transformations in the content of nucleoplasm. Moreover, fusions of FPs with specific cellular protein markers of the nuclear structure−function compartments show potential for noninvasive monitoring of the refractive index in these local nuclear environments.

RESULTS AND DISCUSSION

Here, by utilizing a high temporal and spatial resolution Streak-FLIM technique,[26] we explored whether the fluorescence lifetime of FPs can be used for sensing of fluctuations of the macromolecular environments in the cell interior. A monomeric GFP (derived from *Aequorea victoria*,[40] with the fluorescence peak at ∼508 nm) and tandem dimer tdTomato (a head-to-tail fusion of two monomeric protein units, cloned from Discosoma coral[41] with the fluorescence peak at ∼581 nm) were used as intranuclear FLIM probes. The choice of these FPs was motivated by their chemical stability, extensive FLIM studies reported on them, and by differences in their origin, dimerization, and photophysical properties.[22]

For the FLIM experiments, the populations of asynchronous HeLa cells were transiently transfected with the DNA constructs coding for either GFP (Clontech) or tdTomato (Addgene). Their fluorescence lifetimes in the interphase nuclei were measured and statistically analyzed. Notably, we documented a substantial cell-to-cell variability in the measured fluorescence lifetimes values, which ranged from ∼2.82 to ∼2.97 ns for GFP and from ∼2.85 to ∼3.34 ns for tdTomato. The distributions of fluorescence lifetimes of GFP and tdTomato measured into the nuclei of interphase cells randomly chosen in the cell culture are presented in Figure 1.

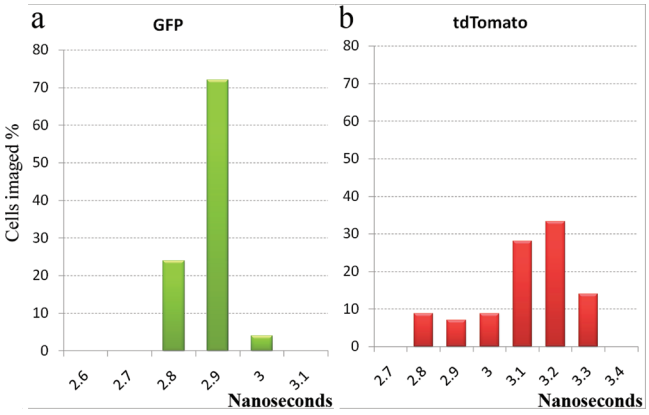

Figure 1. Fluorescence lifetimes of GFP and tdTomato measured in the nuclei of asynchronous HeLa cells. The charts represent distributions of fluorescence lifetimes of (a) GFP and (b) tdTomato measured into the interphase cell nuclei, randomly chosen in the cell culture. The values were rounded to the nearest 10th of a nanosecond.

Taking into account that the molecular structure of the FPs expressed by different cells is identical, the observed cell-to-cell differences in fluorescence lifetime were attributed to different molecular environments, existing in the nucleoplasm of individual cells. The average fluorescence lifetimes for GFP and tdTomato in the interphase cells nuclei were determined to be 2.88 ± 0.05 and 3.14 ± 0.15 ns (mean ± SD), respectively

dx.doi.org/10.1021/cb300065w | *ACS Chem. Biol.* 2012, 7, 1385−1392

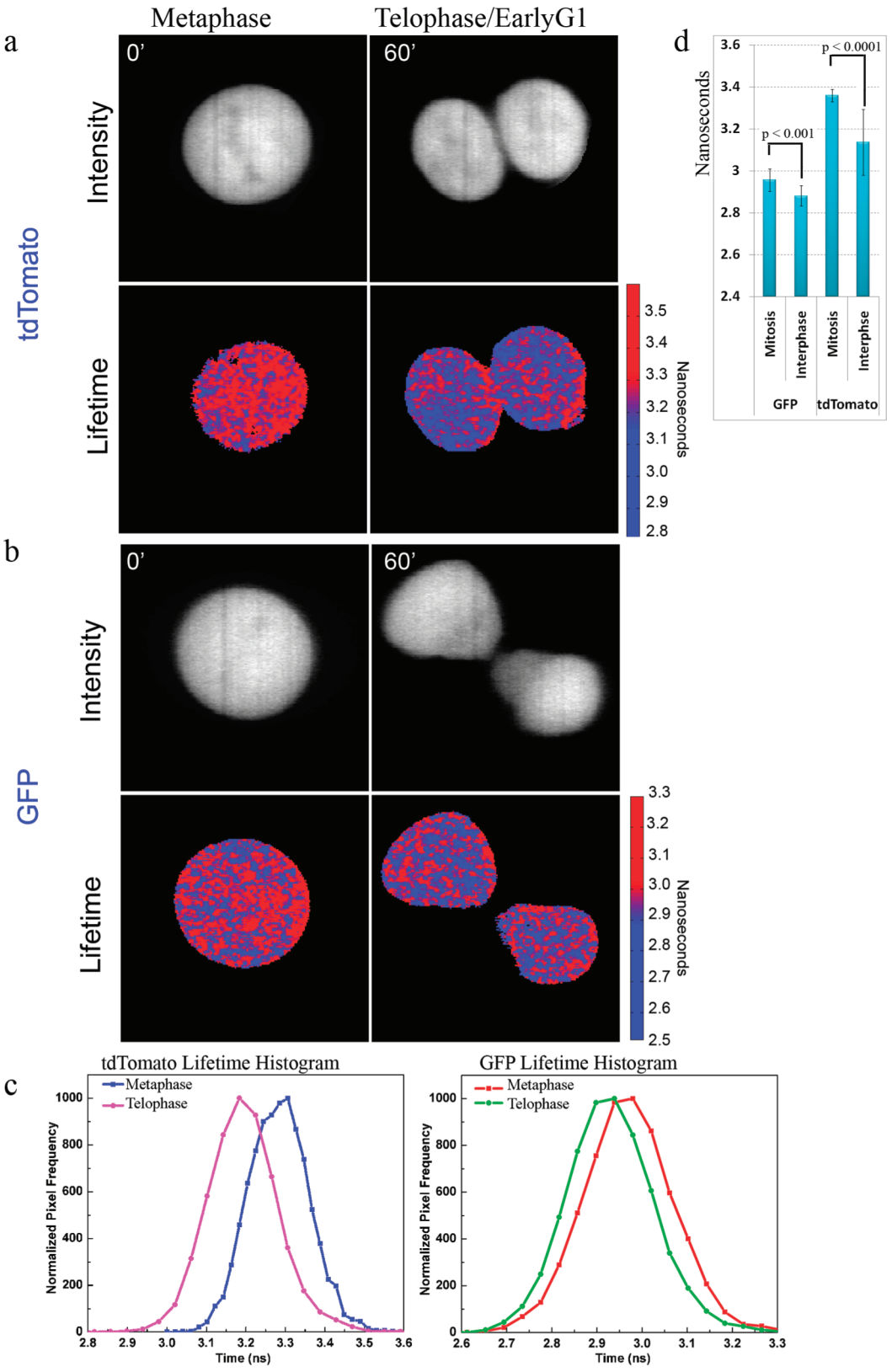

Figure 2. Fluorescence Lifetime of GFP and tdTomato Rapidly Shortens at Mitosis-to-Interphase transition. (a, b) FLIM time lapse tracking of representative cells expressing (a) tdTomato and (b) GFP, throughout the cell division. The mitotic (metaphase) cells expressing FPs were identified by transmission light, and fluorescence lifetime was acquired in these cells in a time-lapse mode throughout the mitotic process. We observed that fluorescence lifetime was constant from metaphase to anaphase and then was rapidly shortened during the telophase. (c) Histograms of tdTomato and GFP fluorescence lifetime distributions in the cells shown in panels a and b. (d) The statistical analysis of fluorescence lifetimes measured in interphase cells nuclei and in mitotic cells. Plot represents averaged values ± SD. The presented *p* values were obtained in an unpaired *t* test.

dx.doi.org/10.1021/cb300065w | *ACS Chem. Biol.* 2012, 7, 1385–1392

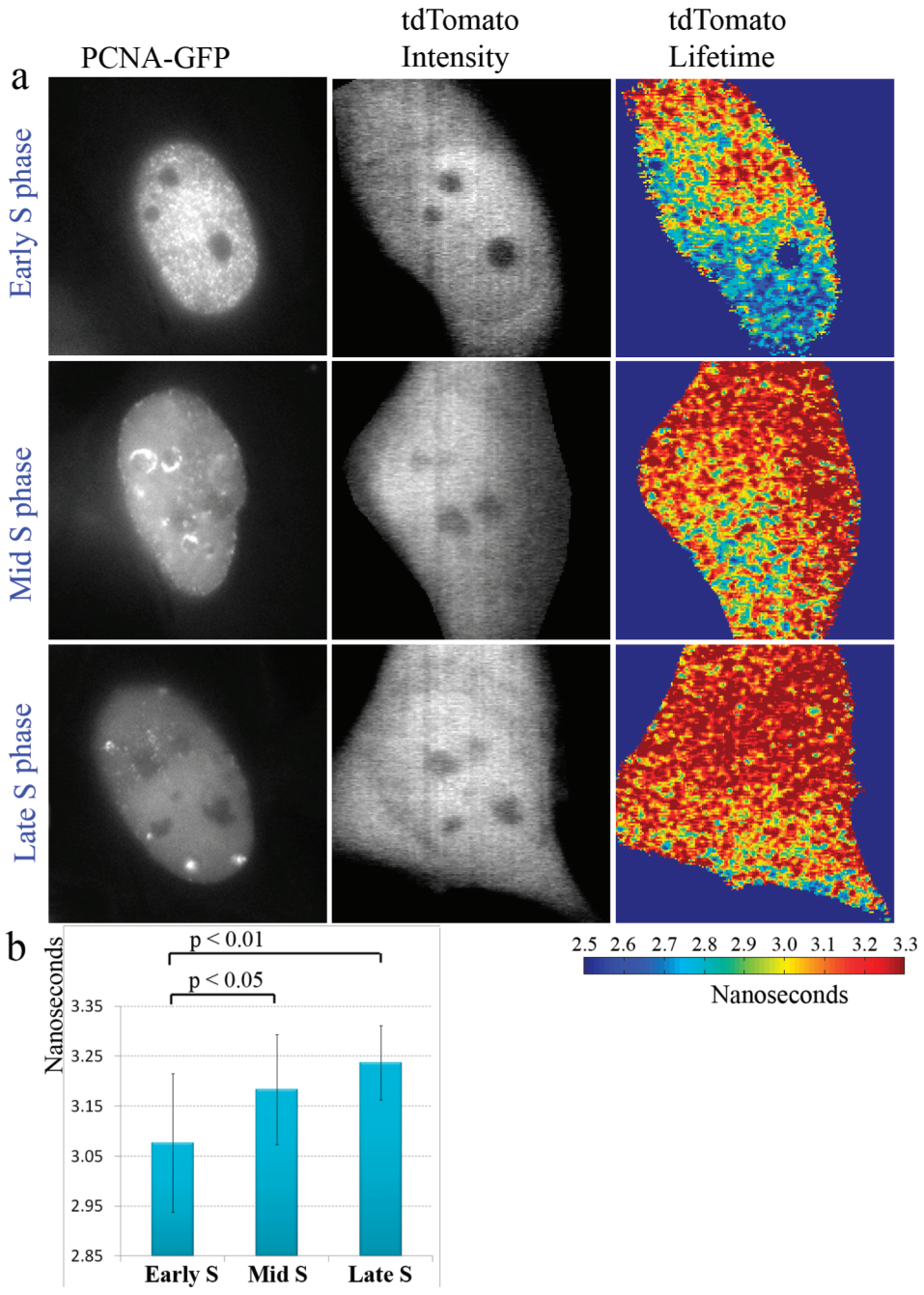

Figure 3. Change of the fluorescence lifetime of the cell nuclear fraction of tdTomato along the S-phase progression. (a) PCNA- GFP and tdTomato (intensity and fluorescence lifetime images) were acquired in the nuclei of same S-phase cells. Early, mid, and late S-phase substages were identified by the PCNA-GFP patterns (left panels, as indicated). (b) Averaged fluorescence lifetime of tdTomato measured in the cell nuclei in early, mid, and late S-phase. Obtained data illustrate a steady increase of the fluorescence lifetime throughout the S-phase. Error bars represent standard deviations. The presented p values were obtained in an unpaired t test.

(Supplementary Figure S2) based on measurements in 26 cells transfected with GFP and 58 cells transfected with tdTomato.

Next, we explored whether a correlation exists between the fluorescence lifetimes of FPs and the cell cycle progression. Throughout the cell cycle, major changes in the nucleoplasmic environment occur during mitosis, when the nuclear envelope disintegrates, contents of nucleoplasm and cytoplasm mix together and then divide between two daughter cells. In order to characterize how these structural transformations impact the fluorescence lifetime of FPs, the mitotic metaphase cells were located by the transmission light and proceeded with FLIM. We found that the fluorescence lifetimes of GFP and tdTomato are significantly longer in the mitotic cells than in the nuclei of the interphase cells. The average lifetimes in the mitotic (metaphase) cells were ~2.96 ± 0.05 ns and ~3.36 ± 0.03 ns for GFP and tdTomato, respectively. Thus, the differences in average fluorescence lifetimes between the metaphase and the interphase cells were ~80 ps for GFP and ~220 ps for tdTomato. We further monitored the metaphase cells until the completion of mitotic process and found that the fluorescence lifetime of both GFP and tdTomato remained constant throughout almost the entire span of mitosis but was rapidly

dx.doi.org/10.1021/cb300065w | ACS Chem. Biol. 2012, 7, 1385–1392

shortened at the final stage of cell division in the telophase (Figure 2a and b). Noticeably, tdTomato fluorescence lifetime values were more reproducible and showed less variability in mitotic cells than in the interphase cells nuclei (Figure 2d). Following the cytokinesis, in the early G1 phase (1−2 h after mitosis), the fluorescence lifetime of FPs was found to be ∼3.13 ± 0.05 and ∼2.83 ± 0.11 ns for tdTomato and GFP, respectively. These values measured in the G1-phase were close to the corresponding average values for the entire population of the interphase cells (Supplementary Figure S2 and Table S1).

We have further monitored the fluorescence lifetime of FPs in cell nuclei during the S-phase progression (Figure 3a), which involves genome duplication and lasts approximately half of the cell cycle in the HeLa cells.[42] In these experiments, cells were co-transfected with tdTomato and another DNA vector, coding for proliferating cell nuclear antigen (PCNA), a cofactor of DNA polymerase, fused to GFP. The cells undergoing the DNA synthesis were identified by the characteristic signal of PCNA-GFP concentrated in the DNA replication sites. The PCNA distribution dynamically changes throughout the S-phase, and we identified cells in the early, mid, or late S-phase [each substage lasts for ∼3−4 h] by their specific PCNA-GFP distribution patterns.[43,44] In order to characterize the fluorescence lifetime of the nucleoplasmic pool of tdTomato throughout the span of the S-phase, 15 or more cells into each substage of the S-phase were statistically analyzed. We preferred such identification of the cells at different subphases of S-phase to chemical cell synchronization protocols, which fail to produce biochemically and morphologically uniform populations of the cultured cells.[45] Also, our experimental design is an attractive alternative to the monitoring of fluorescence lifetime in the same cell for extended periods of interphase, since the repetitive laser excitation in such FLIM experiments negatively influences the cellular viability; meanwhile, unaltered cellular physiology is required for accurate assessment of nucleoplasm throughout the cell development.

Our data obtained for cells expressing both PCNA-GFP and tdTomato indicated a steady increase of the fluorescence lifetime of tdTomato throughout the S-phase. Specifically, in the nuclei of cells exhibiting an early S-phase PCNA-GFP pattern, the lifetime of tdTomato was measured to be 3.10 ± 0.16 ns, whereas in the nuclei of cells featuring mid and late S-phase distribution of PCNA, the corresponding values were ∼3.17 ± 0.14 and 3.23 ± 0.13 ns, respectively (Figure 3, Supplementary Table S1). At the same time, we did not observe apparent changes in the fluorescence lifetime of FPs in cells transiting from the late S- to the G2-phase (cells in the G2 phase were identified by a progressive disappearance of the late S-phase PCNA pattern).

Thus, in the specific examples of the mitotic process, its transition to G1-phase, as well as progression of S-phase, our FLIM experiments documented that these cell cycle events coincide with changes in the fluorescence lifetime of FPs present in the nucleoplasm or mitotic cell protoplasm (Figures 2 and 3 and Supplementary Table S1). Taking into account an inverse correlation of fluorescence lifetime with local refractive index,[24,31−34] we suggest that the fluctuations of macromolecular solutes concentration throughout the cell cycle is a major factor causing the variability of the FPs fluorescence lifetime in the individual cells. In particular, our data imply that the longest lifetime, observed in mitotic cells, corresponds to the lowest intracellular concentration of macromolecules during the cell cycle. A rapid and substantial decrease of the fluorescence lifetime of GFP and tdTomato during the completion of a mitotic division (Figure 2) coincides timely with a decrease in the intracellular volume by a factor of ∼1.4. The ratio between the volumes of mitotic cell and daughter cells can be calculated assuming a preservation of the cell surface area in a process of division, even size for daughter cells and ideal spherical shape of mitotic cells. The ratios between the volumes of mitotic cell and daughter cells were calculated assuming the ideal spherical shape of the mitotic cell. In such an approximation, the surface of the cellular membrane is defined by the sphere surface equation: $S = 4\pi R^2$. Considering that in the process of mitosis the membrane is divided evenly between two daughter cells, $S_1/S_2 = 4\pi R^2/2{\cdot}4\pi r^2$, where S_1 is a surface area of the mitotic cell and S_2 is the combined surface area of the two daughter cells ($S_1 = S_2$); R and r are the radii of the mitotic cell and daughter cells, respectively. Then $R^2 = 2r^2$, $R = r\sqrt{2}$ and the ratio of the volumes of the cells before (V_1) and after (V_2) cell division could be represented (using equation of sphere volume) as follows:

$$V_1/V_2 = \frac{(4/3)\pi R^3}{2{\cdot}(4/3)\pi r^3} = \frac{R^3}{2r^3} = \frac{(\sqrt{2})^3}{2} = \sim 1.\ 41$$

. This postmitotic decrease in the cellular volume results in the same amount of macromolecular solutes becoming confined in a smaller volume, leading to an increase in their concentration, which is consistent with the fluorescence lifetime shortening observed in our experiments (Figure 2).

In the subsequent stages of the interphase, the concentration of macromolecules in the cell nucleus is balanced by the biosynthetic activities increasing the macromolecular concentration and by processes that down-regulate the intranuclear concentration of these solutes such as growth of the nuclear volume and degradation of macromolecules.[10] In this context, it should be noted that the HeLa cell nucleus is nearly doubling its volume during the S-phase, as shown by our and other groups.[2,46] This growth, if not fully compensated by the synthesis of new biomolecules, would lead to a decrease in the concentration of the macromolecular solutes in the nucleoplasm, causing an increase of the fluorescence lifetime of FPs, as observed in our experiments (Figure 3a and b).

Thus, cell-cycle-dependent changes of the concentration of macromolecular solutes in the nucleoplasm can produce a variability of the FP fluorescence lifetimes in the population of the asynchronous cells.

Moreover, cultured cells can exhibit tremendous differences in the cellular growth and synthesis of macromolecules even on the same stage of the cell cycle,[47,48] further contributing to cell-to-cell measurements variability.

Furthermore, in the control experiments, we have verified the fluorescence lifetime response to the changing concentrations of macromolecules in the FPs environment, in both aqueous solutions and the interiors of the cell nuclei. The fluorescence lifetime of GFP was examined in aqueous solutions, with different concentrations of chemically inert protein bovine serum albumin (BSA). Tested BSA concentrations were covering the physiologic range for proteins (most abundant type of cellular in the HeLa cell nucleus (100−150 mg mL^{-1}).[2,15] The fluorescence lifetime of GFP was found to be inversely dependent on the BSA concentration (Supplementary Figure S4), confirming dependence of fluorescence lifetime of FPs on the concentration of the macromolecular solutes.[32] Next, to verify that this dependence is also manifested in live

cells, we have altered the intracellular concentration of macromolecules, forcibly changing the cellular volume by reversible osmotic shock treatment. Alterations to osmotic strength of the cell incubation medium induce water movement in or out of the cell. Under hypotonic incubation conditions, this leads to an increase in the cellular volume and, consequently, to a decrease in the concentration of the intracellular macromolecular solutes, caused by their dilution in the expanding cellular volume. In contrast, upon exposure to a hypertonic medium, cellular volume shrinks, which causes an increase in the concentration of the intracellular and, in particular, intranuclear macromolecules.[49,50] In our experiments, we have found that the fluorescence lifetime of both GFP and tdTomato can be modulated in the same cell nucleus by changing the osmotic strength of the cell incubation solution. Both GFP and tdTomato in the nuclei of the interphase cells manifested an increase in the fluorescence lifetime when the cell medium was exchanged for hypotonic buffer, which caused cell swelling and, correspondingly, a decrease in the concentration of the intranuclear macromolecular solutes. When the same cell was immersed into a hypertonic buffer, this caused an immediate shrinkage of the cell and shortening of the fluorescence lifetime (Supplementary Figure S5). Upon return to initial conditions (incubation in the standard cell medium), the cells recovered the cell cycle progression[50] and manifested fluorescence lifetime values in the previously observed range for nontreated cells. We conclude that these control experiments confirm the sensitivity of FPs lifetime to the saturation of their environment with macromolecules and support FPs feasibility to probe fluctuations of concentration of macromolecules in the nucleoplasm.

Overall, our data demonstrate that FLIM of FPs can be used as a reliable and sensitive tool for probing the macromolecular environment within cells. Evidently, when FPs are tethered to specific proteins, their fluorescence lifetime can be used to probe the refractive index variations at the distinct sites within same cell nucleus. For instance, in a study of van Manen *et al.*, FLIM was used to distinguish between cytosolic and membrane-bound forms of phagocyte receptor fused to GFP, exploiting the difference in the refractive index of cytosol and membrane.[34] In another study of Treanor *et al.*, heterogeneity of fluorescence lifetime of GFP-tagged proteins at the cell surface was revealed and discussed, proposing that FLIM can detect even subtle perturbations of the refractive index and serve as a tool for imaging of the membrane microdomains.[51] Our studies are underway to explore a correlation of distribution of fluorescence lifetime and distinct nuclear domains *via* FLIM of specific proteins fused to FPs.

Conclusions. This study introduces fluorescence lifetimes of fluorescent proteins for monitoring of the nucleoplasmic content. We established the dependence of the fluorescence lifetimes of GFP and tdTomato fluorescent proteins on the cell cycle progression. In particular, the shortest fluorescence lifetime of tdTomato in the cell nucleus was observed in the early S-phase, gradually increasing throughout the span of the S-phase of the cell cycle. The longest fluorescence lifetimes for both GFP and tdTomato were observed in mitosis, being quickly shortened during the cell division. Referring to a known inverse correlation of fluorescence lifetimes with the local refractive index, we suggest that the observed changes of fluorescence lifetime were caused mainly by changes in the concentration of macromolecules in the nucleoplasm throughout the cell cycle.

On the basis of this consideration, we propose that the FLIM of fluorescent proteins offers unparalleled opportunities for sensitive, real-time monitoring of local concentrations of intracellular macromolecules, contributing to the characterization of dynamic molecular organization of the cell. Furthermore, it is important to emphasize that the phenomenon of fluorescence lifetime modulation by the cell-cycle events observed in our study should be considered for a comprehensive interpretation of FLIM data acquired in cycling cells.

METHODS

Cell Culture and Transfection. HeLa cells were grown in glass-bottom dishes (Mattek, Ashland, USA) and cultured in Advanced DMEM (Invitrogen, Carlsbad, USA) supplemented with 2.5% fetal calf serum (Sigma-Aldrich, St. Louis, USA) at 37 °C in a humidified atmosphere containing 5% CO_2. The transfection of tdTomato (Addgene), GFP (Clontech), and PCNA-GFP (Addgene) was performed by using Fugene 6 transfection reagent (Roche) according to manufacturer instructions, and fluorescence lifetime measurements were performed within 24 h after the start of transfection procedure. For the FLIM imaging, morphologically representative cells exhibiting a moderate fluorescence signal were selected. Cells in the mitotic phase were identified by the transmission light imaging.

FLIM Imaging. The FLIM imaging setup (Supplementary Figure S1a) is equipped with a streak camera system (C9136 FLIM system, Hamamatsu Photonics) coupled to an inverted fluorescence microscope setup (Nikon TE2000U). The C9136 FLIM system is capable of fluorescence lifetime measurements in the spectral range from UV to near-infrared. The light from the picosecond pulse diode laser head (Hamamatsu Photonics, PLP-10) with excitation wavelength of 470 nm was scanned by a pair of Galvo mirrors and directed into the left side port of the microscope and focused onto the sample with a 60x/NA1.4 oil-immersion objective for single-photon excitation. The emitted fluorescence signal is collected by the same objective, passes the dichroic mirror and the laser cut filter (500 nm long pass), and then is detected by the streak camera.

The electrical signal from the PLP controller passes through the synchronous delay generator, which is in the EXT.TRIG mode before triggering the streak camera through a Streak camera controller (Delay and Trigger Unit in Supplementary Figure S1a). The galvo mirrors, streak camera, and CCD camera are controlled by the control unit. The Streak-FLIM setup is characterized by a high temporal resolution (less than 20 ps), broad range of lifetime measurements (1 ns−10 ms), short acquisition time (40−300 s/frame at various experimental conditions), and high 2D spatial resolution (up to 0.2 μm).

In the Streak-FLIM optics, one of the Galvo mirrors scans the excitation spot across the sample along a single line (x axis) while the streak camera collects the fluorescence decay from every point along this line, which produces a 2D streak image with space and time as the ordinate and abscissa, respectively. A multimedia file demonstrating the schematics of the Hamamatsu Streak camera is available online (http://learn.hamamatsu.com/tutorials/java/streakcamera/). Another Galvo mirror scans the excitation spot synchronously along the y direction. This process gives a stack of streak images that contains complete information on the fluorescence intensity as well as spatial and temporal information from the sample. Numerical processing of all of these raw streak images pixel-by-pixel gives the final FLIM image of the sample. In this study, AquaCosmos software (Hamamatsu Photonics, K.K.) was used for FLIM data acquisition and analysis. An example of FPs fluorescence decay and instrument response function (IRF) acquired and analyzed using C9136 FLIM system with AquaCosmos software is shown in Supplementary Figure S1b.

It should be noted that although 470 nm is not the optimal wavelength to excite fluorescence of tdTomato [absorption peak is at 552 nm[52]], the FP does absorb light at this wavelength. Provided that tdTomato is the brightest among all currently available FPs,[41] the 470 nm laser line could be efficiently used to obtain FLIM data. When the

FLIM was performed in cells co-transfected with PCNA-GFP, the tdTomato signal was selected using the additional 600 nm long pass filter in front of the streak camera. In GFP/tdTomato co-transfection experiments the appropriate controls (cells transfected with GFP only) were used to ensure complete cutoff of the GFP signal under conditions of tdTomato FLIM.

The constancy and reproducibility of FLIM data were verified by repetitive measurements of fluorescence lifetime in the same cells. Representative Supplementary Figure S3 shows a time-lapse sequence of a mitotic cell acquired with 20 min intervals and two daughter cells resulted from this cell division. The difference in measured fluorescence lifetimes was insignificant until the cell divided.

The lifetime fitting was performed using a single exponential model for each pixel in the image. The FLIM images presented in the manuscript were obtained using in-house software, developed with Matlab (PFL V1.0) for the raw streak image processing, FLIM image display, histogram and other analysis.

Statistical analysis was performed by using the unpaired *t* test incorporated in SigmaPlot software.

■ ASSOCIATED CONTENT

Supporting Information

Details on FLIM instrumentation, design and results of the control experiments, as well as statistically analyzed fluorescence lifetimes values measured at specific stages of the cell cycle. This material is available free of charge *via* the Internet at http://pubs.acs.org.

■ AUTHOR INFORMATION

Corresponding Author

*E-mail: pnprasad@acsu.buffalo.edu; jlqu@szu.edu.cn.

Notes

The authors declare no competing financial interest.

■ ACKNOWLEDGMENTS

This work was supported by a grant from the John R. Oishei Foundation.

■ REFERENCES

(1) Prasad, P. N. (2003) *Introduction to Biophotonics*, Wiley-Interscience, Hoboken, NJ.

(2) Pliss, A., Kuzmin, A. N., Kachynski, A. V., and Prasad, P. N. (2010) Nonlinear optical imaging and Raman microspectrometry of the cell nucleus throughout the cell cycle. *Biophys. J. 99*, 3483−3491.

(3) Pliss, A., Kuzmin, A. N., Kachynski, A. V., and Prasad, P. N. (2010) Biophotonic probing of macromolecular transformations during apoptosis. *Proc. Natl. Acad. Sci. U.S.A. 107*, 12771−12776.

(4) Misteli, T. (2008) Cell biology: Nuclear order out of chaos. *Nature 456*, 333−334.

(5) Minton, A. P. (2006) How can biochemical reactions within cells differ from those in test tubes? *J. Cell Sci. 119*, 2863−2869.

(6) Misteli, T. (2007) Beyond the sequence: cellular organization of genome function. *Cell 128*, 787−800.

(7) Eden, E., Geva-Zatorsky, N., Issaeva, I., Cohen, A., Dekel, E., Danon, T., Cohen, L., Mayo, A., and Alon, U. (2011) Proteome half-life dynamics in living human cells. *Science 331*, 764−768.

(8) Gregory, T. R. (2001) Coincidence, coevolution, or causation? DNA content, cell size, and the C-value enigma. *Biol. Rev. Cambridge Philos. Soc. 76*, 65−101.

(9) Umen, J. G. (2005) The elusive sizer. *Curr Opin Cell Biol 17*, 435−441.

(10) Alon, U. (2007) *An Introduction to Systems Biology Design Principles of Biological Circuits*, Chapman & Hall-CRC, Boca Raton, FL.

(11) Nurse, P. (2000) A long twentieth century of the cell cycle and beyond. *Cell 100*, 71−78.

(12) Tseng, Y., Lee, J. S., Kole, T. P., Jiang, I., and Wirtz, D. (2004) Micro-organization and visco-elasticity of the interphase nucleus revealed by particle nanotracking. *J. Cell Sci. 117*, 2159−2167.

(13) Grunwald, D., Martin, R. M., Buschmann, V., Bazett-Jones, D. P., Leonhardt, H., Kubitscheck, U., and Cardoso, M. C. (2008) Probing intranuclear environments at the single-molecule level. *Biophys. J. 94*, 2847−2858.

(14) Bacher, C. P., Reichenzeller, M., Athale, C., Herrmann, H., and Eils, R. (2004) 4-D single particle tracking of synthetic and proteinaceous microspheres reveals preferential movement of nuclear particles along chromatin - poor tracks. *BMC Cell Biol. 5*, 45.

(15) Handwerger, K. E., Cordero, J. A., and Gall, J. G. (2005) Cajal bodies, nucleoli, and speckles in the Xenopus oocyte nucleus have a low-density, sponge-like structure. *Mol. Biol. Cell 16*, 202−211.

(16) Rowat, A. C., Lammerding, J., Herrmann, H., and Aebi, U. (2008) Towards an integrated understanding of the structure and mechanics of the cell nucleus. *Bioessays 30*, 226−236.

(17) Choi, W., Fang-Yen, C., Badizadegan, K., Oh, S., Lue, N., Dasari, R. R., and Feld, M. S. (2007) Tomographic phase microscopy. *Nat. Methods 4*, 717−719.

(18) Koberna, K., Ligasova, A., Malinsky, J., Pliss, A., Siegel, A. J., Cvackova, Z., Fidlerova, H., Masata, M., Fialova, M., Raska, I., and Berezney, R. (2005) Electron microscopy of DNA replication in 3-D: evidence for similar-sized replication foci throughout S-phase. *J. Cell Biochem. 94*, 126−138.

(19) Pliss, A., Malyavantham, K., Bhattacharya, S., Zeitz, M., and Berezney, R. (2009) Chromatin dynamics is correlated with replication timing. *Chromosoma 118*, 459−470.

(20) Ma, H., Samarabandu, J., Devdhar, R. S., Acharya, R., Cheng, P. C., Meng, C., and Berezney, R. (1998) Spatial and temporal dynamics of DNA replication sites in mammalian cells. *J. Cell Biol. 143*, 1415−1425.

(21) Pakhomov, A. A., and Martynov, V. I. (2008) GFP family: structural insights into spectral tuning. *Chem. Biol. 15*, 755−764.

(22) Shaner, N. C., Steinbach, P. A., and Tsien, R. Y. (2005) A guide to choosing fluorescent proteins. *Nat. Methods 2*, 905−909.

(23) Wallrabe, H., and Periasamy, A. (2005) Imaging protein molecules using FRET and FLIM microscopy. *Curr. Opin. Biotechnol. 16*, 19−27.

(24) Berezin, M. Y., and Achilefu, S. (2010) Fluorescence lifetime measurements and biological imaging. *Chem. Rev. 110*, 2641−2684.

(25) Levitt, J. A., Matthews, D. R., Ameer-Beg, S. M., and Suhling, K. (2009) Fluorescence lifetime and polarization-resolved imaging in cell biology. *Curr. Opin. Biotechnol. 20*, 28−36.

(26) Periasamy, A., Clegg, R. M. (2010) *FLIM Microscopy in Biology and Medicine*, Taylor & Francis, Boca Raton, FL.

(27) Bastiaens, P. I., and Squire, A. (1999) Fluorescence lifetime imaging microscopy: spatial resolution of biochemical processes in the cell. *Trends Cell Bio.l 9*, 48−52.

(28) Tadrous, P. J. (2000) Methods for imaging the structure and function of living tissues and cells: 2. Fluorescence lifetime imaging. *J. Pathol. 191*, 229−234.

(29) Toptygin, D. (2003) Effects of the solvent refractive index and its dispersion on the radiative decay rate and extinction coefficient of a fluorescent solute. *J. Fluoresc. 13*, 201−219.

(30) Strickler, S. J., and Berg, R. A. (1962) Relationship between absorption intensity and fluorescence lifetime of molecules. *J. Chem. Phys. 37*, 814−822.

(31) Borst, J. W., Hink, M. A., van Hoek, A., and Visser, A. J. (2005) Effects of refractive index and viscosity on fluorescence and anisotropy decays of enhanced cyan and yellow fluorescent proteins. *J. Fluoresc. 15*, 153−160.

(32) Suhling, K., Siegel, J., Phillips, D., French, P. M., Leveque-Fort, S., Webb, S. E., and Davis, D. M. (2002) Imaging the environment of green fluorescent protein. *Biophys. J. 83*, 3589−3595.

(33) Tregidgo, C., Levitt, J. A., and Suhling, K. (2008) Effect of refractive index on the fluorescence lifetime of green fluorescent protein. *J. Biomed. Opt. 13*, 031218.

(34) van Manen, H. J., Verkuijlen, P., Wittendorp, P., Subramaniam, V., van den Berg, T. K., Roos, D., and Otto, C. (2008) Refractive index sensing of green fluorescent proteins in living cells using fluorescence lifetime imaging microscopy. *Biophys. J. 94*, L67−L69.
(35) Bizzarri, R., Serresi, M., Luin, S., and Beltram, F. (2009) Green fluorescent protein based pH indicators for in vivo use: a review. *Anal. Bioanal. Chem. 393*, 1107−1122.
(36) Kneen, M., Farinas, J., Li, Y. X., and Verkman, A. S. (1998) Green fluorescent protein as a noninvasive intracellular pH indicator. *Biophys. J. 74*, 1591−1599.
(37) Llopis, J., McCaffery, J. M., Miyawaki, A., Farquhar, M. G., and Tsien, R. Y. (1998) Measurement of cytosolic, mitochondrial, and Golgi pH in single living cells with green fluorescent proteins. *Proc. Natl. Acad. Sci. U.S.A. 95*, 6803−6808.
(38) Tantama, M., Hung, Y. P., and Yellen, G. (2011) Imaging intracellular pH in live cells with a genetically encoded red fluorescent protein sensor. *J. Am. Chem. Soc. 133*, 10034−10037.
(39) Nakabayashi, T., Wang, H. P., Kinjo, M., and Ohta, N. (2008) Application of fluorescence lifetime imaging of enhanced green fluorescent protein to intracellular pH measurements. *Photochem. Photobiol. Sci. 7*, 668−670.
(40) Shimomura, O., Johnson, F. H., and Saiga, Y. (1962) Extraction, purification and properties of aequorin, a bioluminescent protein from the luminous hydromedusan, Aequorea. *J. Cell. Comp. Physiol. 59*, 223−239.
(41) Shaner, N. C., Campbell, R. E., Steinbach, P. A., Giepmans, B. N. G., Palmer, A. E., and Tsien, R. Y. (2004) Improved monomeric red, orange and yellow fluorescent proteins derived from Discosoma sp red fluorescent protein. *Nat. Biotechnol. 22*, 1567−1572.
(42) Dimitrova, D. S., and Berezney, R. (2002) The spatio-temporal organization of DNA replication sites is identical in primary, immortalized and transformed mammalian cells. *J. Cell. Sci. 115*, 4037−4051.
(43) Nakayasu, H., and Berezney, R. (1989) Mapping replicational sites in the eucaryotic cell nucleus. *J. Cell Biol. 108*, 1−11.
(44) Somanathan, S., Suchyna, T. M., Siegel, A. J., and Berezney, R. (2001) Targeting of PCNA to sites of DNA replication in the mammalian cell nucleus. *J. Cell Biochem. 81*, 56−67.
(45) Cooper, S. (2003) Rethinking synchronization of mammalian cells for cell cycle analysis. *Cell. Mol. Life Sci. 60*, 1099−1106.
(46) Walter, J., Schermelleh, L., Cremer, M., Tashiro, S., and Cremer, T. (2003) Chromosome order in HeLa cells changes during mitosis and early G1, but is stably maintained during subsequent interphase stages. *J. Cell Biol. 160*, 685−697.
(47) Snijder, B., and Pelkmans, L. (2011) Origins of regulated cell-to-cell variability. *Nat. Rev. Mol. Cell Biol. 12*, 119−125.
(48) Spiller, D. G., Wood, C. D., Rand, D. A., and White, M. R. (2010) Measurement of single-cell dynamics. *Nature 465*, 736−745.
(49) Ho, S. N. (2006) Intracellular water homeostasis and the mammalian cellular osmotic stress response. *J. Cell Physiol. 206*, 9−15.
(50) Koberna, K., Stanek, D., Malinsky, J., Eltsov, M., Pliss, A., Ctrnacta, V., Cermanova, S., and Raska, I. (1999) Nuclear organization studied with the help of a hypotonic shift: its use permits hydrophilic molecules to enter into living cells. *Chromosoma 108*, 325−335.
(51) Treanor, B., Lanigan, P. M., Suhling, K., Schreiber, T., Munro, I., Neil, M. A., Phillips, D., Davis, D. M., and French, P. M. (2005) Imaging fluorescence lifetime heterogeneity applied to GFP-tagged MHC protein at an immunological synapse. *J. Microsc. 217*, 36−43.
(52) Campbell, R. E., Tour, O., Palmer, A. E., Steinbach, P. A., Baird, G. S., Zacharias, D. A., and Tsien, R. Y. (2002) A monomeric red fluorescent protein. *Proc. Natl. Acad. Sci. U.S.A. 99*, 7877−7882.